Metal content along the quasar main sequence

Paola Marziani[1]

and several collaborators of "the extreme team"

A. del Olmo[2], C. A. Negrete[3], D. Dultzin[3], M. D'Onofrio[4], S. Panda[5], M. Śniegowka[6], E. Bon[7], N. Bon[7]

graduate students: A. Deconto Machado[2], T. Buendia[3], K. Garnica Luna[3], A. Floris[4]

[1]INAF - Osservatorio Astronomico di Padova, Padova, Italy

[2]Instituto de Astrofísica de Andalucía (CSIC), Granada, Spain

[3]Instituto de Astronomía, UNAM, México, D.F., Mexico

[4]Dipartimento di Fisica ed Astronomia "Galileo Galilei", U. di Padova, Padova, Italy

[5]Laboratório Nacional de Astrofísica, Itajubá, Brazil

[6]Tel Aviv University, Tel Aviv, Israel

[7]Astronomomical Observatory, Belgrade, Serbia

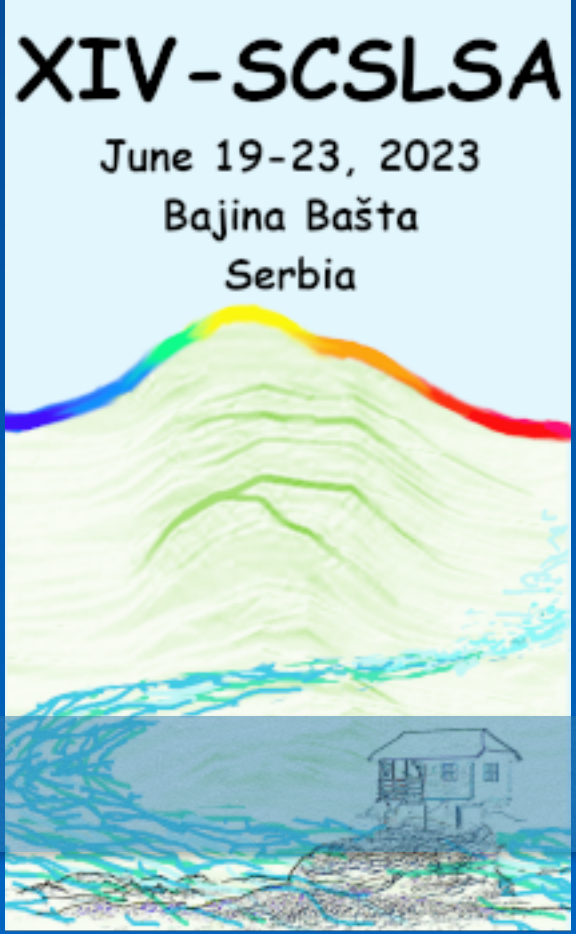

June 12, 2023

A main sequence for quasars

❊ MS≡Eigenvector 1; optical plane
anti-correlation between strength of FeIIλ4570 and FWHM of Hβ ($R_{\rm FeII}$ = FeIIλ4570/Hβ)
(e.g.: Boroson & Green 1992; Gaskell 1985; Sulentic et al. 2000a,b; Shen & Ho 2014; Rakshit et al. 2020; Wu & Shen 2023

❊ Spectral types can be identified as well as and two main populations of type-1 AGN: Pop. A and Pop. B (high- and low-$L/L_{\rm Edd}$) , extreme Pop. A ⇛ candidate super Eddington
Sulentic et al. 2002; Sulentic et al. 2011; Shen & Ho 2014; Super-Eddington: Wang et al. 2013; Marziani & Sulentic 2014; Du et al. 2018

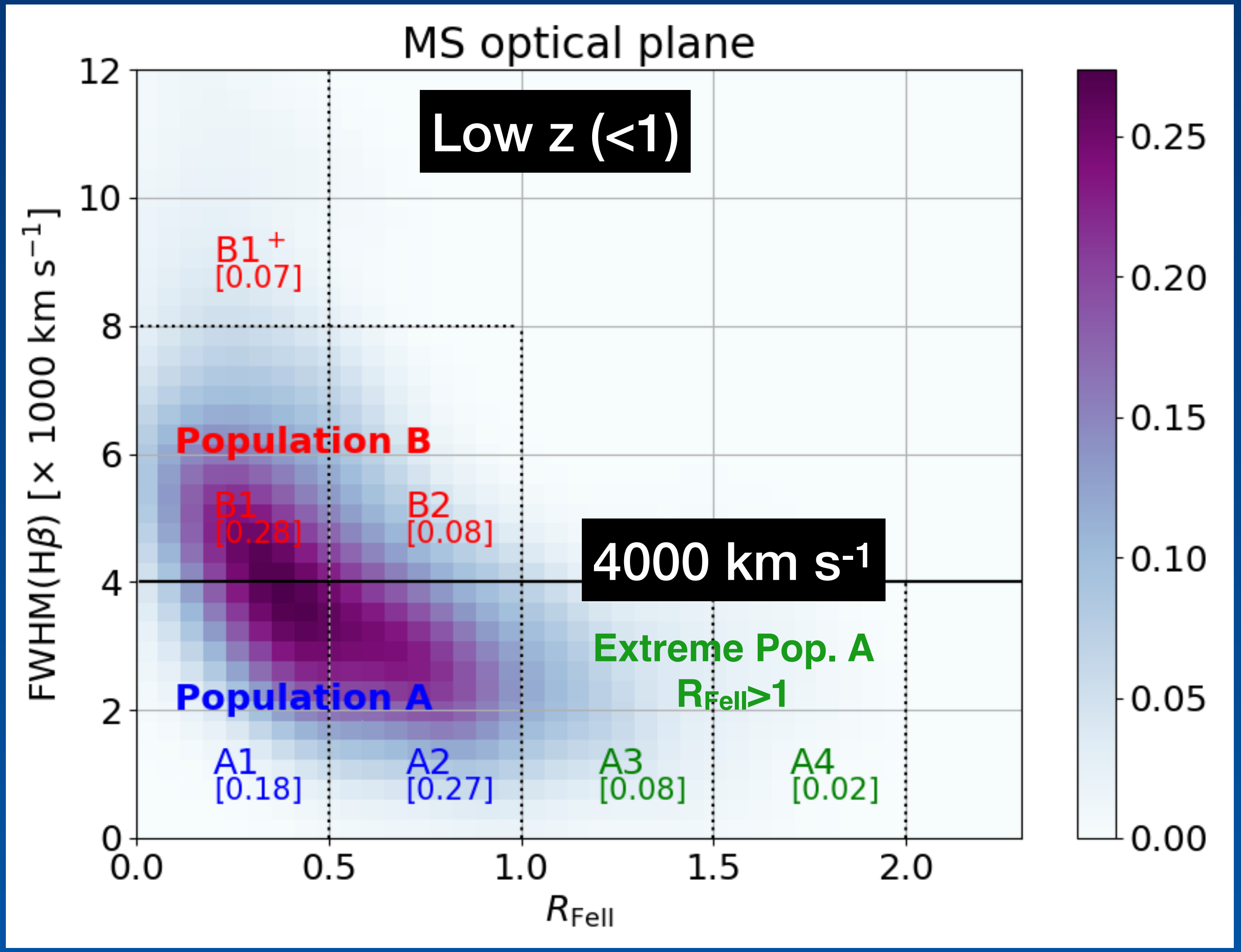

Zamfir et al. 2010: n ~ 470, z<0.7 from SDSS DR 5, log L ~ 45.5 [erg/s]

❊ Type-1 AGN multifrequency diversity is organized long a sequence driven by Eddington ratio / orientation

4DE1 of Sulentic et al. 2000a; summary table in Fraix-Burnet et al. 2017; $L/L_{\rm Edd}$: Marziani et al. 2001; Boroson 2002; Shen & Ho 2014; Sun & Shen 2015; Panda et al. 2019

Constrains SED, wind/virialized emission, accretion process

The Main Sequence as an evolutionary scheme

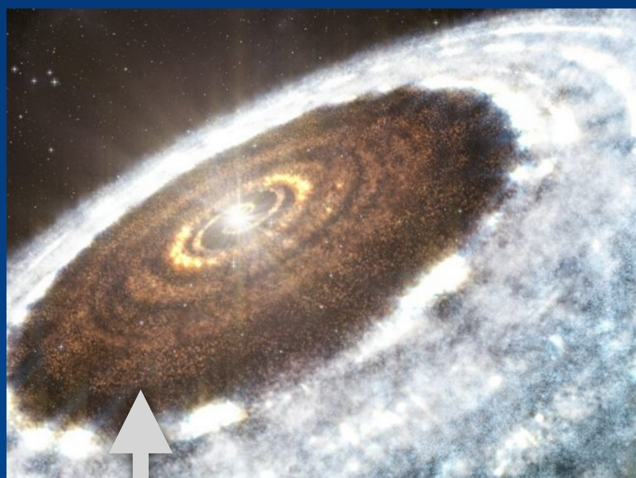

From young / rejuvenated (NLSy1s in extreme Population A, including jetted sources) to massive, low Eddington radiators, “starving”

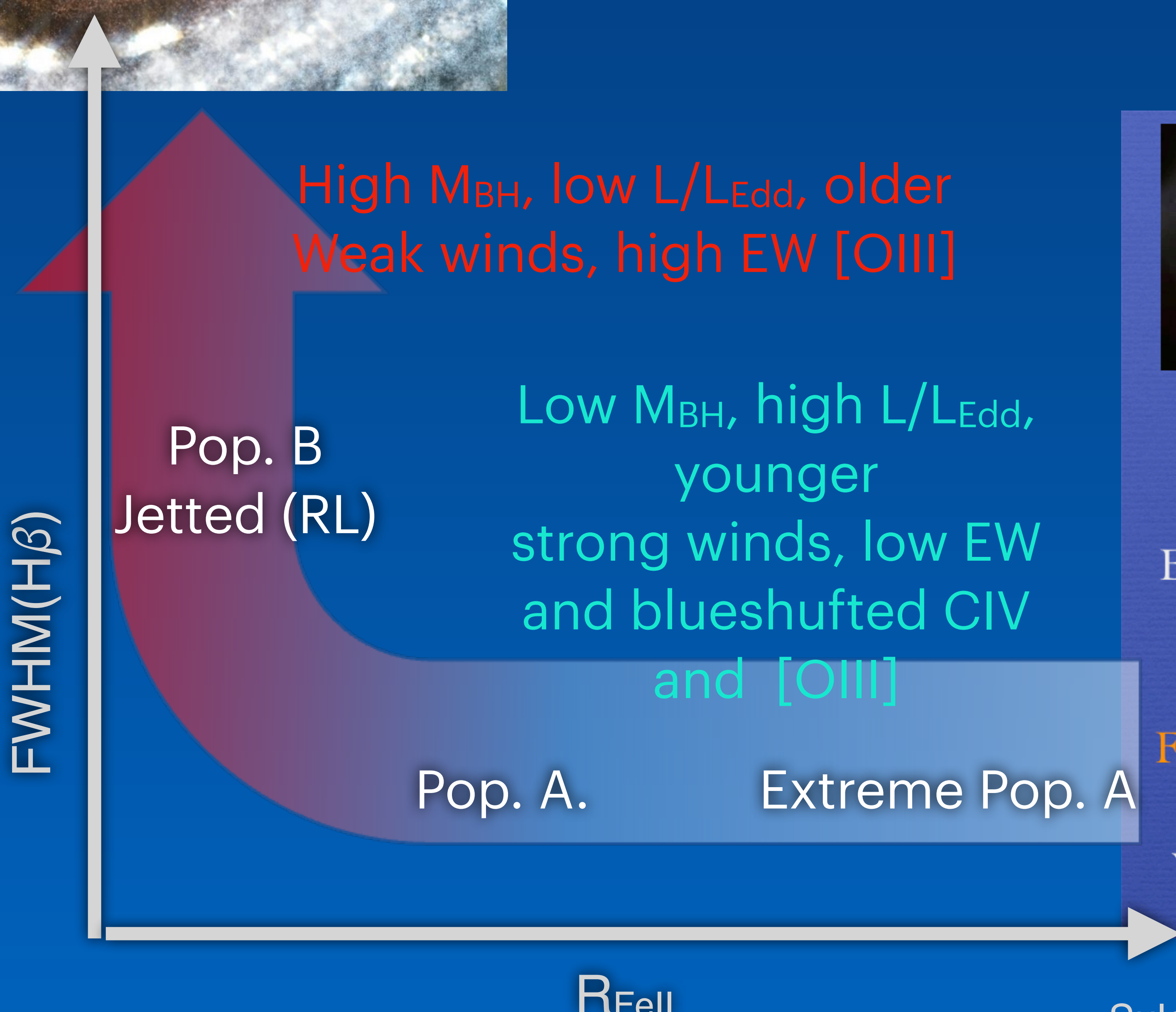

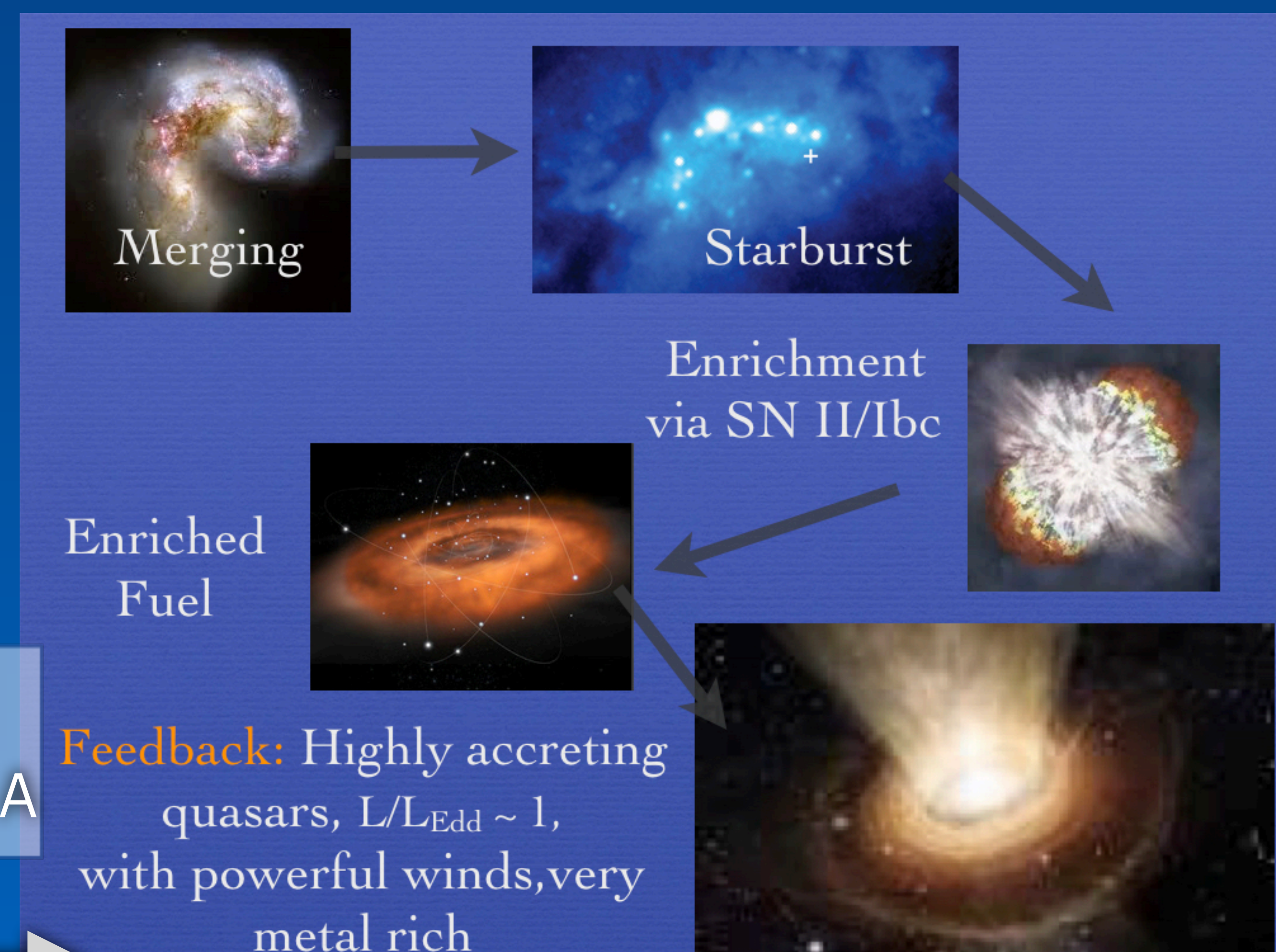

Sulentic et al. 2000; Mathur 2000; Komossa et al. 2006; Xu & Komossa 2008; Berton et al. 2017; Fraix-Burnet et al. 2017

HST/FOS-based composites along the MS

- Composite spectra from a sample of ~130 radio-quiet HST/FOS and matching high S/N optical data, covering CIV, and Hβ for each object, z < 0.9, log L ~ 45-47 [erg s^{-1}]
  Sulentic et al. 2007

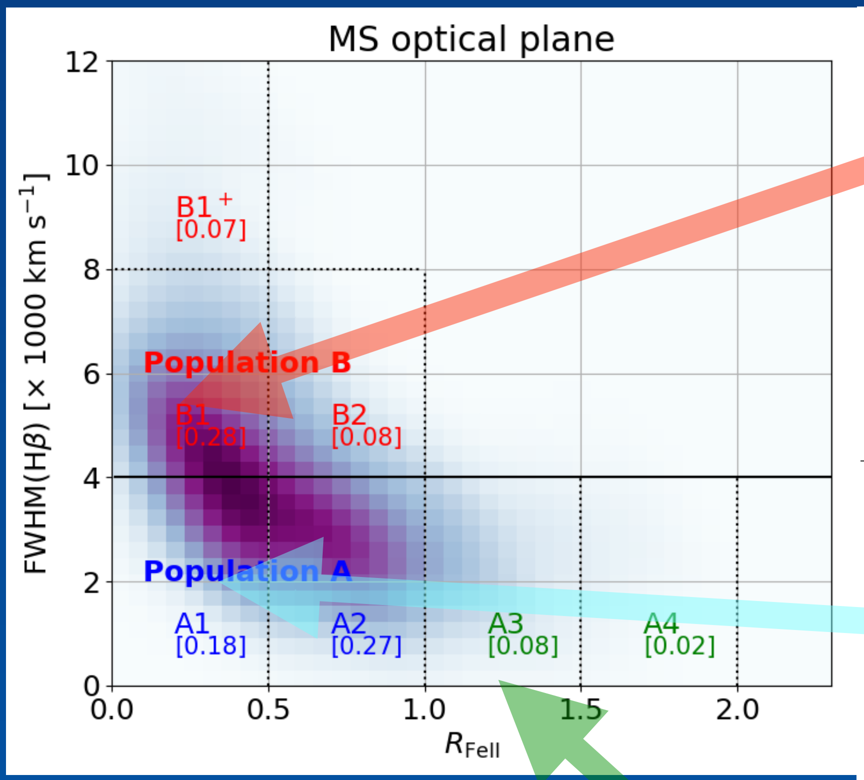

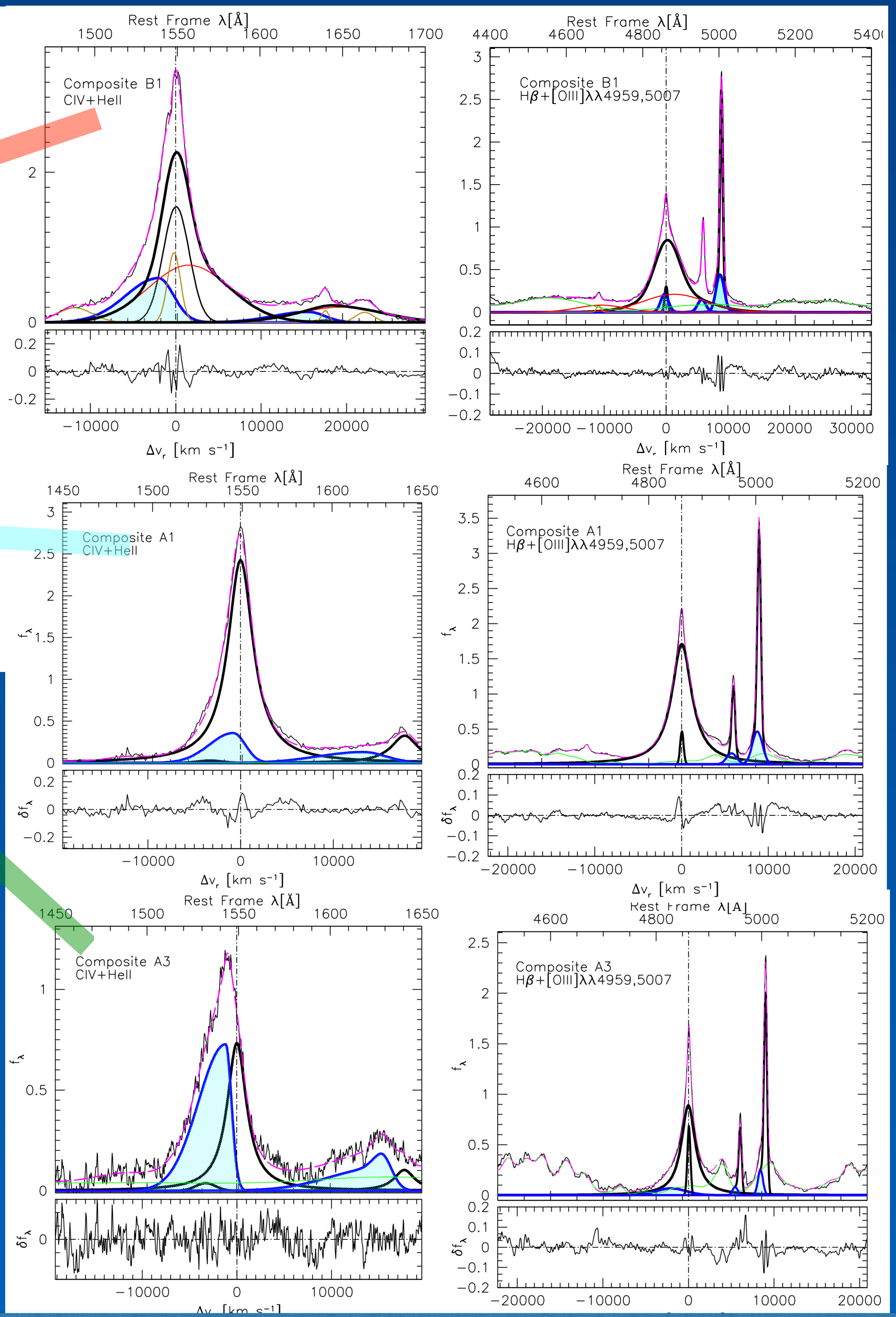

- Multicomponent analysis: line profiles modeled by virialized (Pop. A unshifted, symmetric Lorentzian; Pop. B double Gaussian; broad and very broad component) + blue shifted outflow emission (skew Gaussian) in high ionization CIVλ1549 (BLR)
  Sulentic et al. 2007; Marziani et al. 2010; c.f. Leighly & Moore 2004; Sulentic et al. 2007; Richards et al. 2011; for [OIII], Zamanov et al. 2002, Komossa et al. 2008, Zhang et al. 2011

Outflow ubiquitous but prominent at high $R_{\rm FeII}$ (extreme Pop. A)

Estimation of metallicity Z, density n_H and ionization U

- Coverage of a parameter space in n_H, ionization parameter U, metallicity Z, SED with CLOUDY 17.01
- Diagnostic line ratios CIVλ1549/HeIIλ1640 AlIII λ1860/HeIIλ1640 (SiIV+OIV])λ1400/ HeIIλ1640 dependent on metallicity Z on a monotonic way
- Comparison between arrays of ~10^4 predicted intensity ratios from photoionisation simulations using CLOUDY 17.02, and measured ratios sensitive to n_H, U, and Z
Ferland et al. 2017

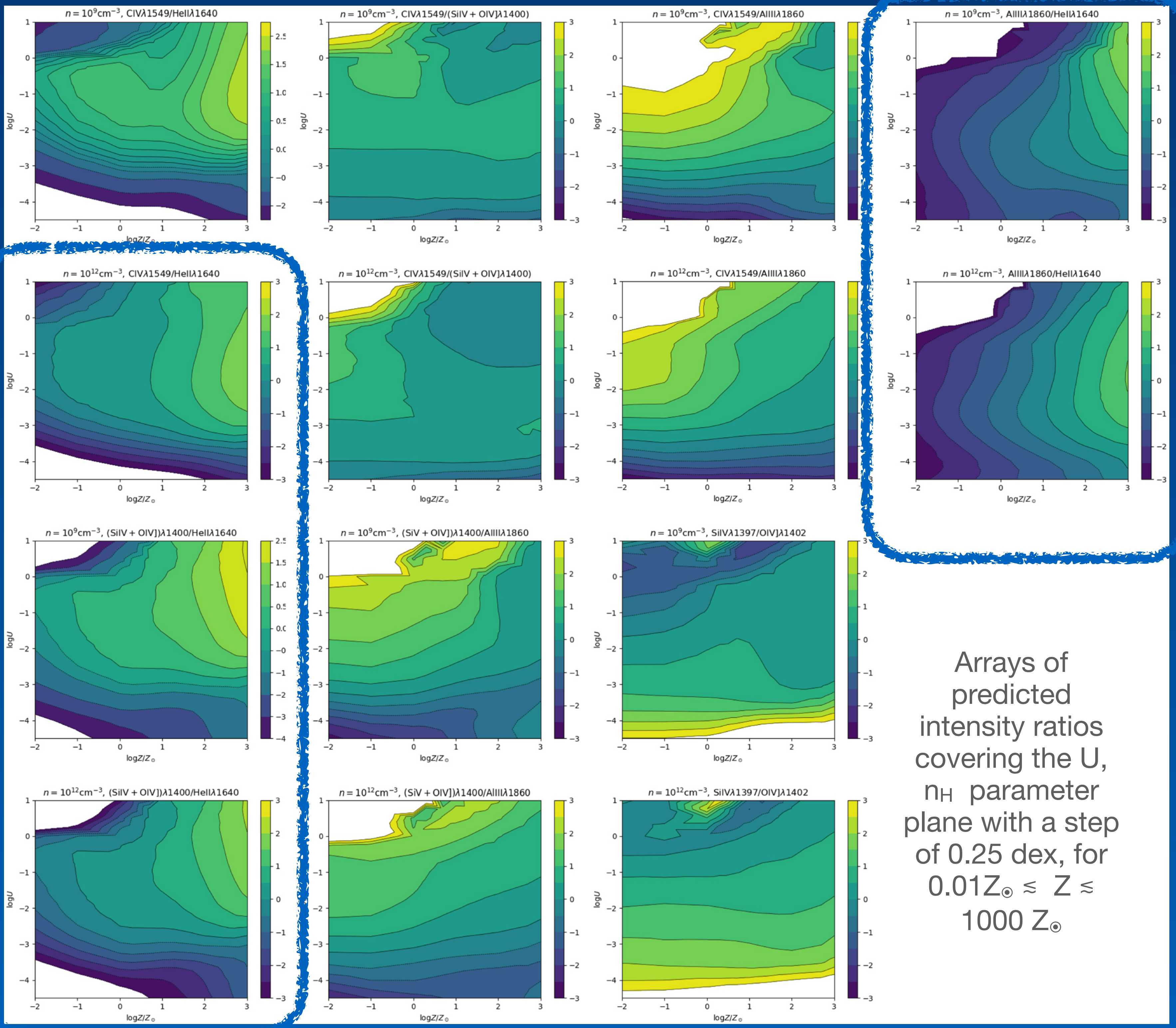

Arrays of predicted intensity ratios covering the U, n_H parameter plane with a step of 0.25 dex, for $0.01 Z_\odot \lesssim Z \lesssim 1000 Z_\odot$

$Z \pm \delta Z$ from $\chi^2(n, U, Z)$ within $n\sigma$ from minimum

Sniegowska et al. 2021 and in preparation; Marziani et al. 2020; Garnica et al. 2022

Measurement of emission line: profile ratios

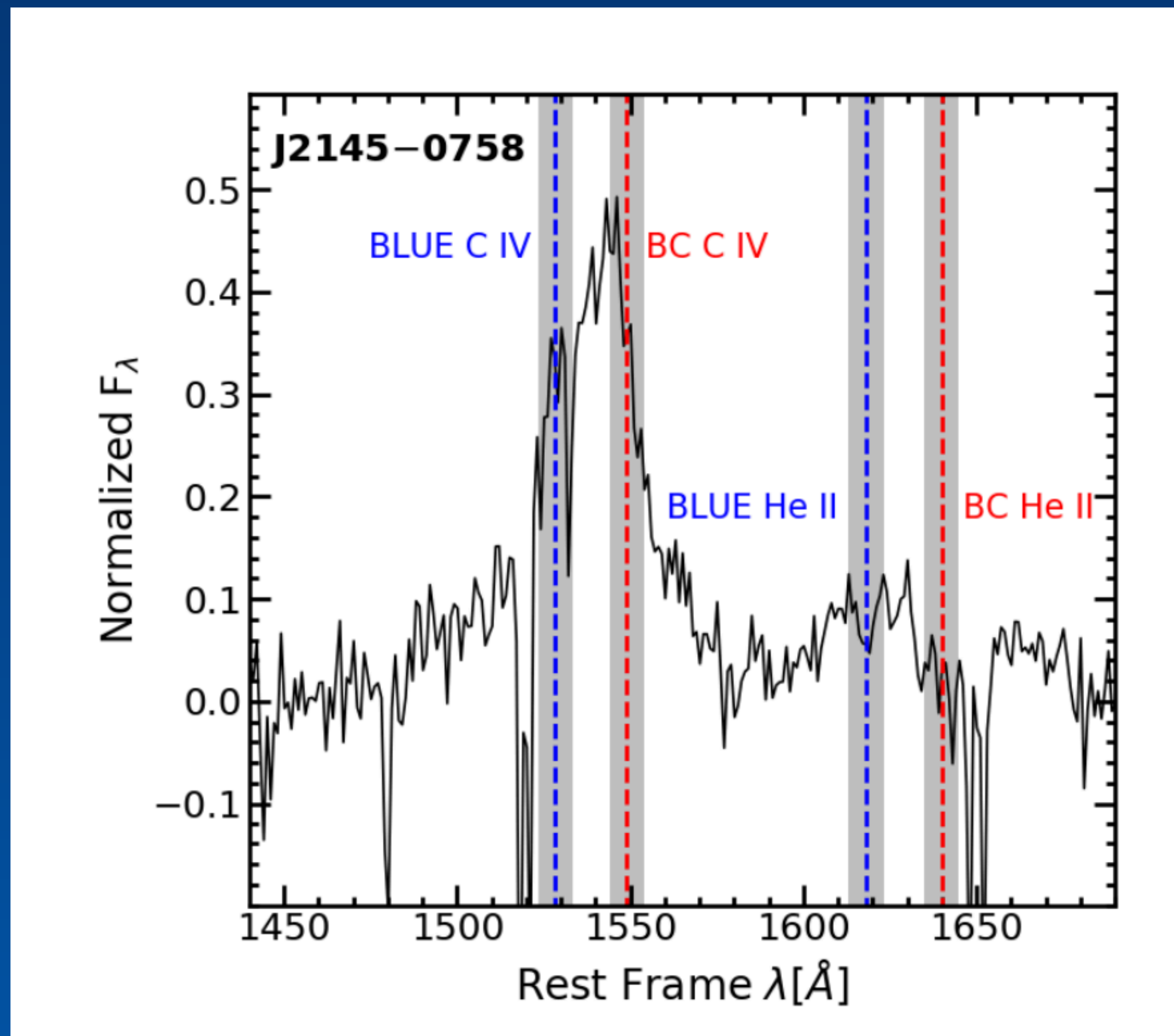

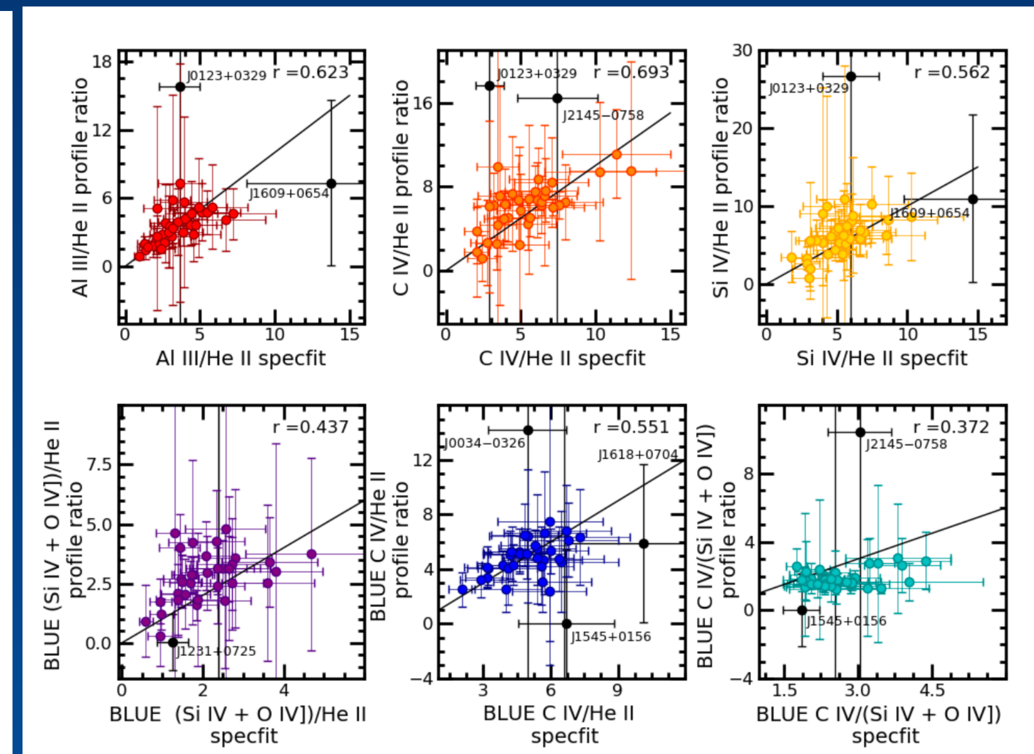

- Typical uncertainties are $\delta \log Z \approx 0.3$ (excluding rare outliers)

Garnica et al. 2022

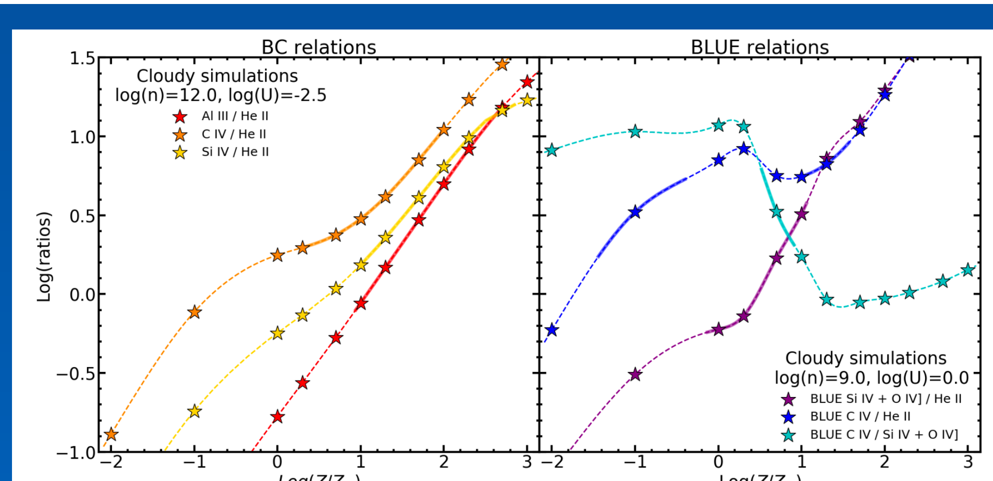

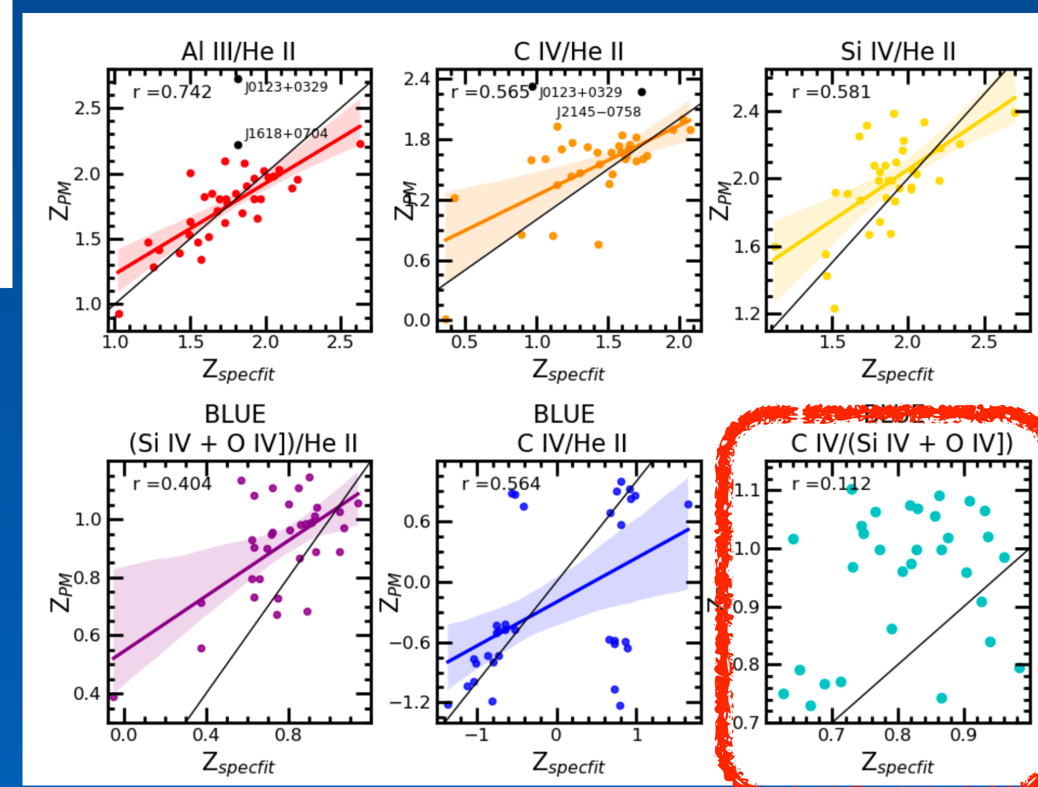

Results consistent with line multi-component analysis

Jetted Population B: broad Balmer profiles, low R_{FeII}

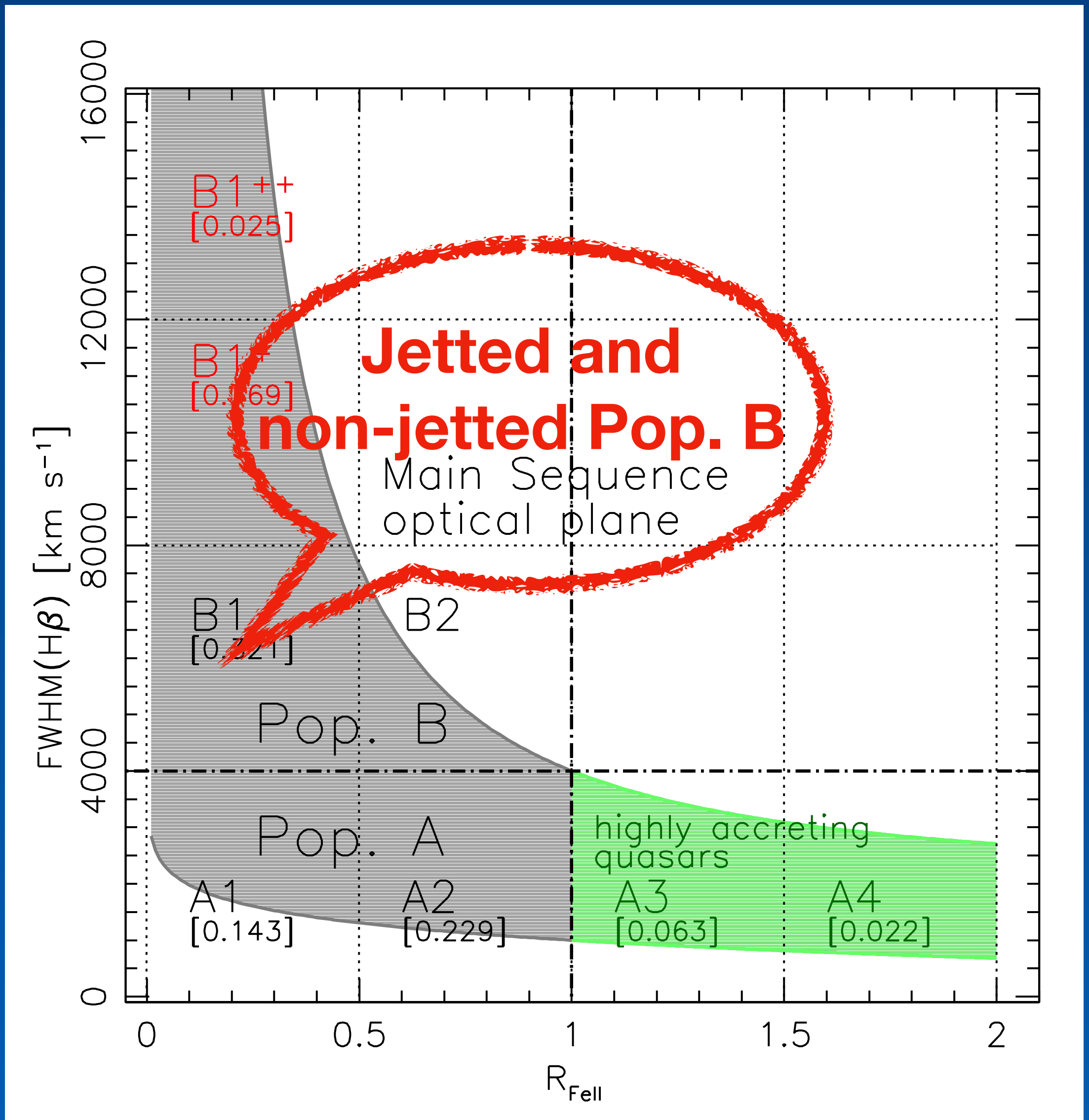

Low Eddington ratio

NGC 1275 ≡ Perseus A

- Weak BLR emission with superimposed outflow emission in CIV and [OIII]
  Punsly et al. 2018

$$\frac{L(\mathrm{C\,IV})}{L(\mathrm{H}\beta)} = 0.3 - 0.8, \; \frac{L(\mathrm{P}\alpha)}{L(\mathrm{H}\beta)} = 0.6 - 1.1,$$
$$\frac{L(\mathrm{Fe\,II})}{L(\mathrm{H}\beta)} < 0.3,$$
$$\frac{L(\mathrm{He\,II}\lambda1640)}{L(\mathrm{C\,IV})} = 0.5 - 1.0.$$

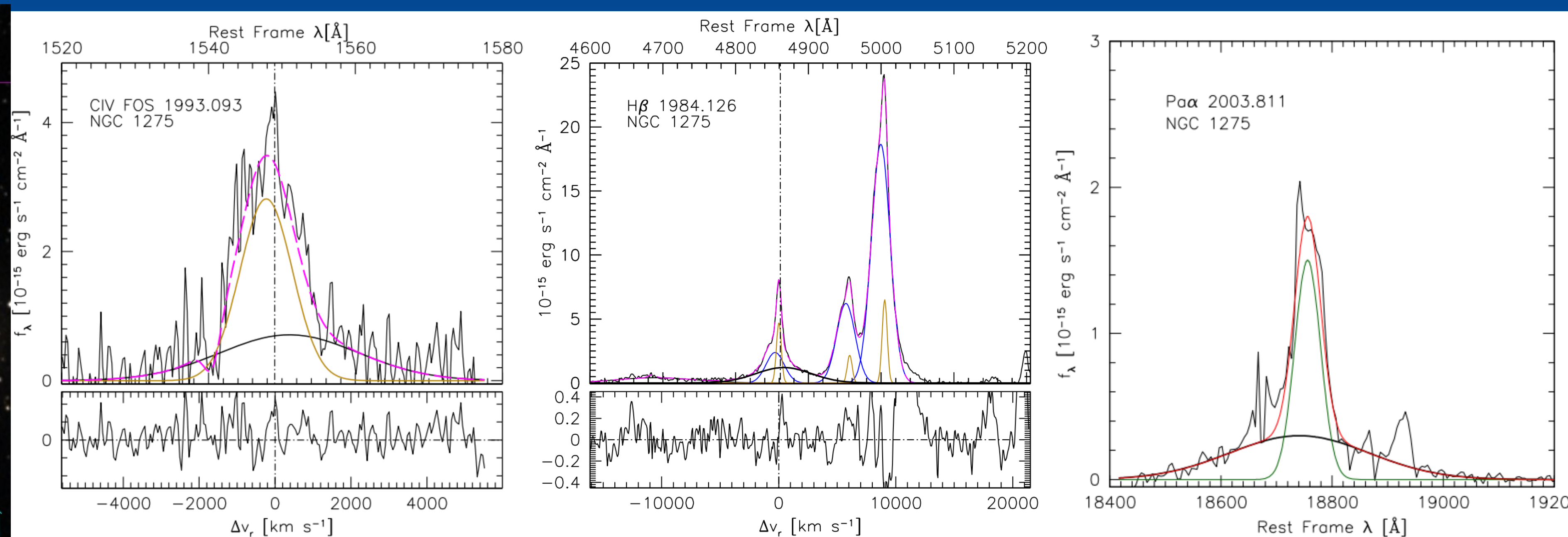

low FeII, low CIV

see Marziani et al. 2023a for a survey of type-1 AGN in cluster of galaxies

NGC 1275: solar or slightly subsolar metallicity, 0.1 $Z_{\odot} \lesssim Z \lesssim 1\ Z_{\odot}$

- Exploration of a parameter subspace in n_H, ionization parameter U, N_H, metallicity Z, using a carefully defined SED with CLOUDY 17.01

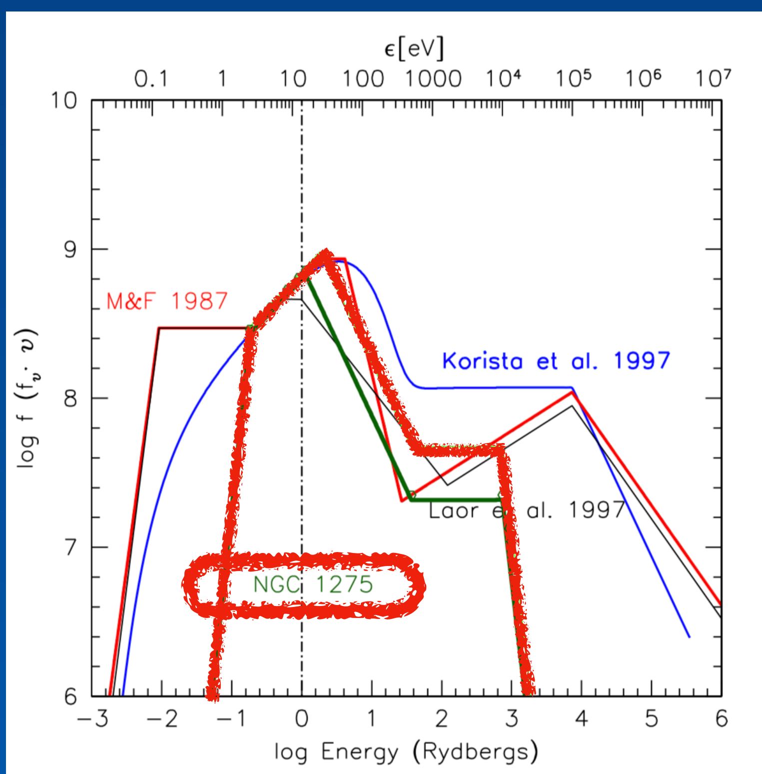

- Moderate density $n_H \sim 10^{10}$ cm^{-3}, and column density $N_H \sim 10^{22-23}$ cm^{-2}

Table 2
CLOUDY Simulations: NGC 1275

1	2	3	4	5	6	7	8	9	10	11
Z	$\log n$	$\log N_H$	$\log r$	$\log U$	$\log L(H\beta)$	C IV/Hβ	Pα/Hβ	He II/C IV	Fe II/Hβ	Conformance
Metalicity	Number Density cm^{-3}	Column Density cm^{-2}	Radius cm	Ionization Parameter	Luminosity erg s^{-1}	Target 0.3–0.8	Target 0.6–1.1	Target 0.5–1.0	Target <0.3	
0.1	9.75	22.7	16.5	−1.24	40.76	1.63	0.99	0.44	0.03	No
0.1	9.75	23.3	16.5	−1.24	40.80	1.47	1.09	0.43	0.06	No
0.1	9.75	22.7	16.75	−1.74	40.76	1.63	0.99	0.44	0.03	No
0.1	9.75	23.3	16.75	−1.74	40.80	1.47	1.09	0.43	0.06	No
0.1	9.75	22.7	17.0	−2.24	40.76	1.63	0.99	0.44	0.03	No
0.1	9.75	23.3	17.0	−2.24	40.80	1.47	1.09	0.43	0.06	No
0.1	10.0	22.7	16.5	−1.49	40.81	0.63	0.92	0.99	0.02	Yes
0.1	10.0	23.3	16.5	−1.49	40.84	0.59	1.01	0.97	0.05	Yes
0.1	10.0	22.7	16.75	−1.99	40.81	0.63	0.91	0.99	0.02	Yes
0.1	10.0	23.3	16.75	−1.99	40.84	0.59	1.01	0.97	0.05	Yes
0.1	10.0	22.7	17.0	−2.49	40.81	0.63	0.91	0.99	0.02	Yes
0.1	10.0	23.3	17.0	−2.49	40.84	0.59	1.01	0.97	0.05	Yes
0.1	10.25	22.7	16.5	−1.74	40.87	0.20	0.84	2.64	0.02	No
0.1	10.25	23.3	16.5	−1.74	40.89	0.19	0.93	2.59	0.04	No
0.1	10.25	22.7	16.75	−2.24	40.87	0.20	0.84	2.64	0.02	No
0.1	10.25	23.3	16.75	−2.24	40.89	0.19	0.93	2.59	0.04	No
0.1	10.25	22.7	17.0	−2.74	40.87	0.20	0.84	2.64	0.02	No
0.1	10.25	23.3	17.0	−2.74	40.89	0.19	0.93	2.59	0.04	No
0.1	10.5	22.7	16.5	−1.99	40.93	0.06	0.77	8.22	0.02	No
0.1	10.5	23.3	16.5	−1.99	40.94	0.05	0.87	8.08	0.03	No
0.1	10.5	22.7	16.75	−2.49	40.93	0.06	0.77	8.22	0.02	No
0.1	10.5	23.3	16.75	−2.49	40.94	0.05	0.87	8.08	0.03	No
0.1	10.5	22.7	17.0	−2.99	40.93	0.06	0.77	8.22	0.02	No
0.1	10.5	23.3	17.0	−2.99	40.94	0.05	0.87	8.08	0.03	No
1.0	9.75	22.7	16.5	−1.24	40.75	11.8	0.33	0.07	0.04	No
1.0	9.75	23.3	16.5	−1.24	40.83	9.77	0.35	0.07	0.07	No
1.0	9.75	22.7	16.75	−1.74	40.82	7.67	0.60	0.08	0.08	No
1.0	9.75	23.3	16.75	−1.74	40.89	6.49	0.54	0.08	0.11	No
1.0	9.75	22.7	17.0	−2.24	40.76	3.85	1.02	0.18	0.19	No
1.0	9.75	23.3	17.0	−2.24	40.78	3.65	1.05	0.18	0.27	No
1.0	10.0	22.7	16.5	−1.49	40.71	11.2	0.32	0.07	0.05	No
1.0	10.0	23.3	16.5	−1.49	40.77	9.72	0.36	0.07	0.08	No
1.0	10.0	22.7	16.75	−1.99	40.85	5.20	0.52	0.11	0.07	No
1.0	10.0	23.3	16.75	−1.99	40.88	4.84	0.56	0.11	0.11	No
1.0	10.0	22.7	17.0	−2.49	40.79	1.91	0.97	0.32	0.22	No
1.0	10.0	23.3	17.0	−2.49	40.81	1.84	1.00	0.32	0.22	No
1.0	10.25	22.7	16.5	−1.74	40.69	9.33	0.35	0.09	0.06	No
1.0	10.25	23.3	16.5	−1.74	40.73	8.40	0.34	0.09	0.09	No
1.0	10.25	22.7	16.75	−2.24	40.81	3.55	0.55	0.17	0.08	No
1.0	10.25	23.3	16.75	−2.24	40.86	3.15	0.54	0.17	0.11	No
1.0	10.25	22.7	17.0	−2.74	40.83	0.76	0.91	0.73	0.12	Yes
1.0	10.25	23.3	17.0	−2.74	40.85	0.73	0.94	0.73	0.18	Yes
1.0	10.5	22.7	16.5	[illegible]	[illegible]	[illegible]	[illegible]	[illegible]	[illegible]	No
1.0	10.5	23.3	16.5	−1.99	40.68	6.86	0.41	0.13	0.11	No
1.0	10.5	22.7	16.75	−2.49	40.82	1.85	0.54	0.32	0.08	No
1.0	10.5	23.3	16.75	−2.49	40.83	1.81	0.54	0.32	0.12	No
1.0	10.5	22.7	17.0	−2.99	40.88	0.23	0.84	2.09	0.10	No
1.0	10.5	23.3	17.0	−2.99	40.89	0.22	0.84	2.09	0.15	No

Approach must depend on spectral type, individual peculiarities

Population B radio-quiet and jetted (radio-loud) composites

- Decomposition BC / VBC

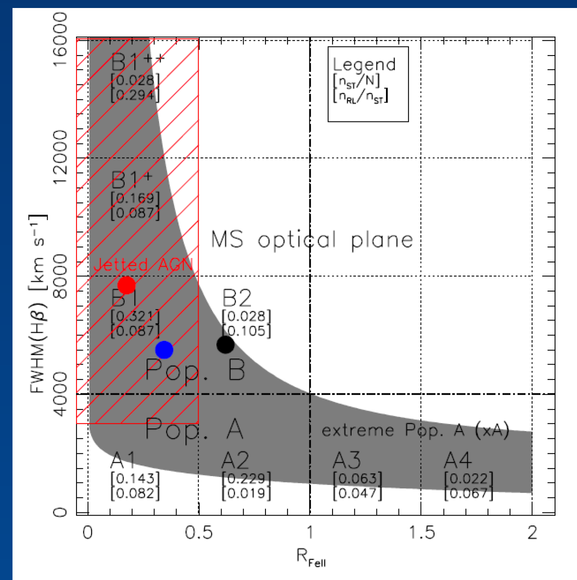

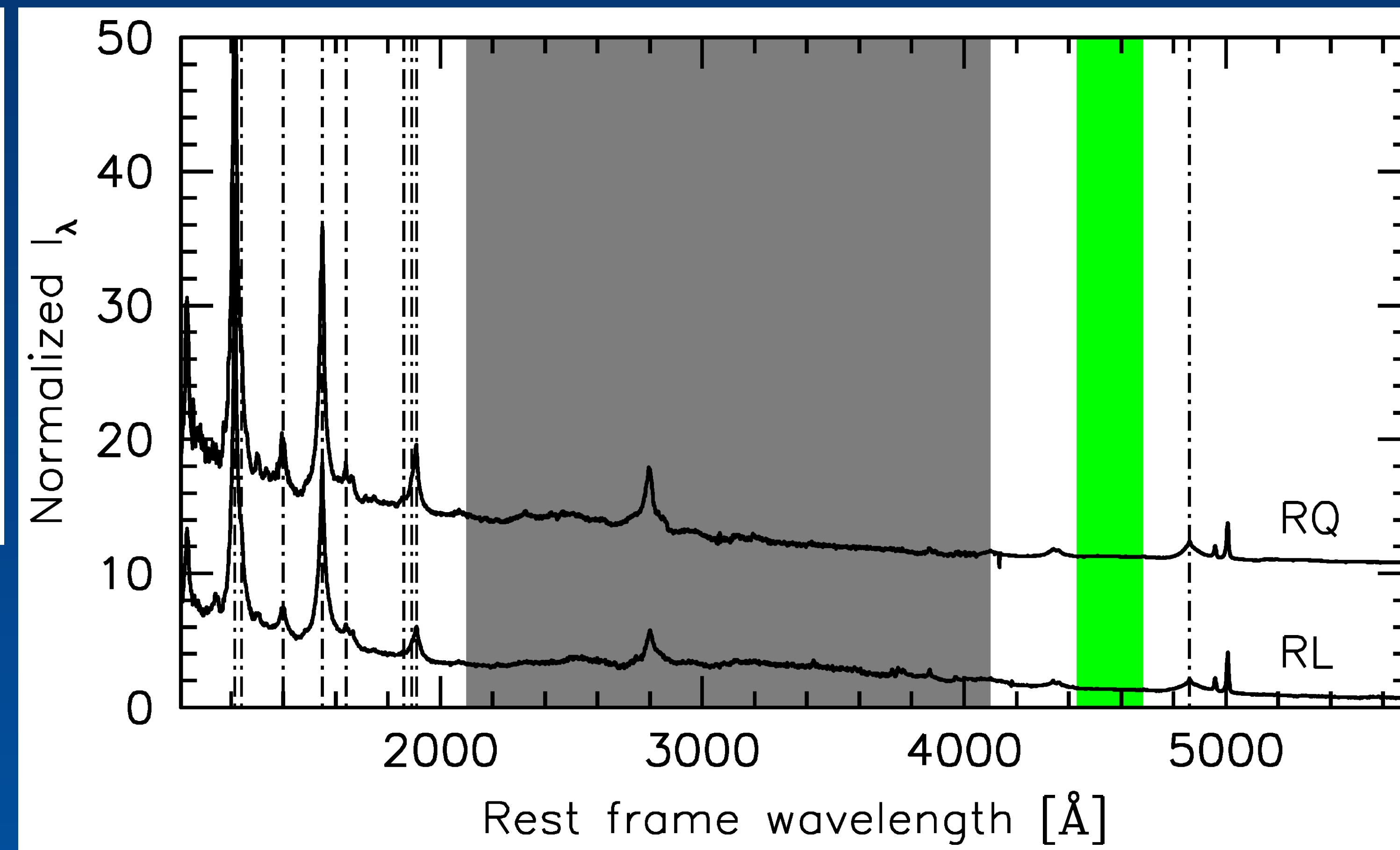

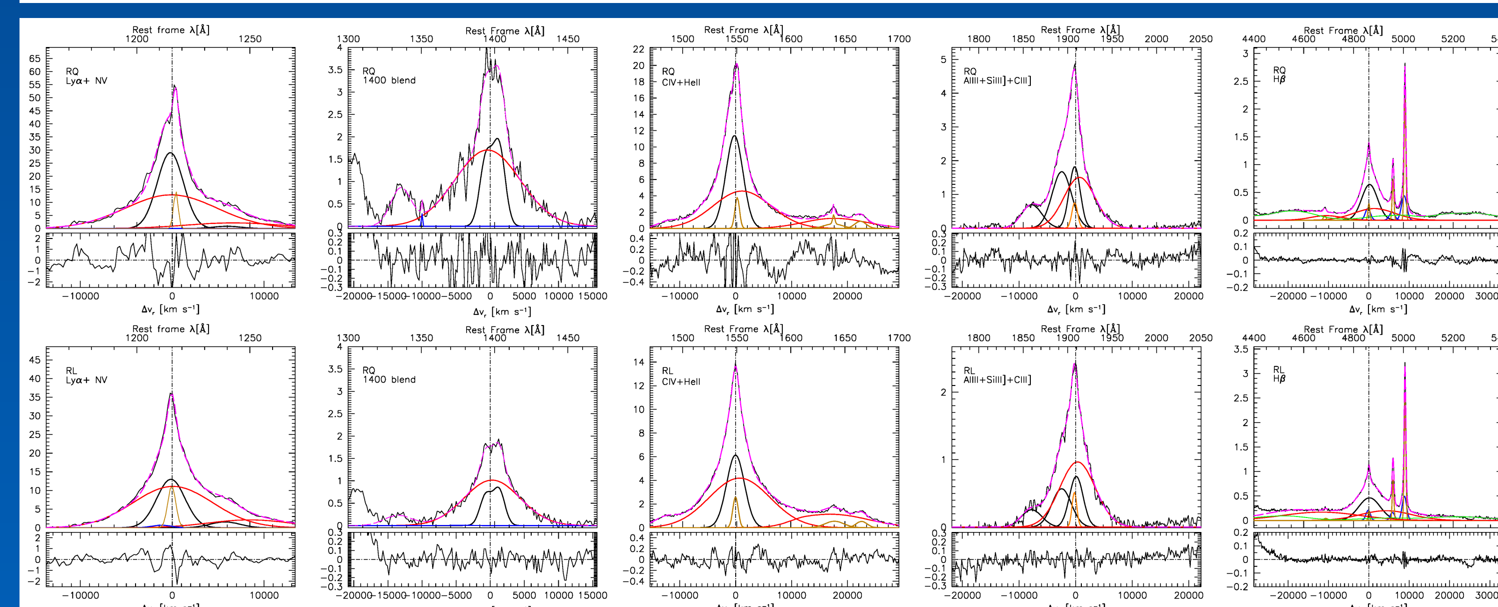

NV/CIV
CIV/HeIIλ1640
CIV/Hβ
SiIV+OIV]/CIV
SiIV+OIV]/HeIIλ1640
AlIII/CIV
AlIII/SiIII]
FeII/Hβ ~ 0.17 (RL), ~ 0.34 (RQ)
SiIII]/CIII]
HeIIλ4686/Hβ

low prominence of metal lines (with respect to H and He lines)

Jetted: definitely sub solar metallicities; RQ: solar

- Systematic differences between BC and VBC (BLR and inner VBLR), consistent with virial velocity field and stratification in Pop. B
- “Stratification” complicates estimates; a locally optimised emitting cloud model is needed

Table 2. Derived values of U, Z, $n_{\rm H}$ and 1σ ranges [a].

Class	Region	log U	Δ log U	log Z	Δ log Z	log$n_{\rm H}$	Δ log $n_{\rm H}$
RQ	Tot.	−2.25	−2.25–−2.25	−0.30	−0.70–0.00	9.50	8.50–9.75
RQ	BLR	−2.25	−2.25–−1.75	0.30	−0.70–1.00	10.25	9.25–10.75
RQ	VBLR	0.00	0.00–0.00	0.70	0.70–0.70	9.50	9.50–9.75
RL	Tot.	[illegible]	−2.00–−0.75	−1.30	−2.00–−1.30	8.75	7.00–9.75
RL	BLR	−1.50	−2.00–−0.75	−1.70	−2.00– −1.00	10.25	8.75–10.50
RL	VBLR	−0.75	−1.25–−0.25	−2.00	−2.00–−1.70	7.75	7.00–10.25

[a]: ionization parameter U, abundance Z in solar units, and hydrogen particle density $n_{\rm H}$ in units of cm^{-3}. The ranges are defined by the limiting elements of the model grid that are compatible with the minimum χ^2_ν within 1σ confidence level.

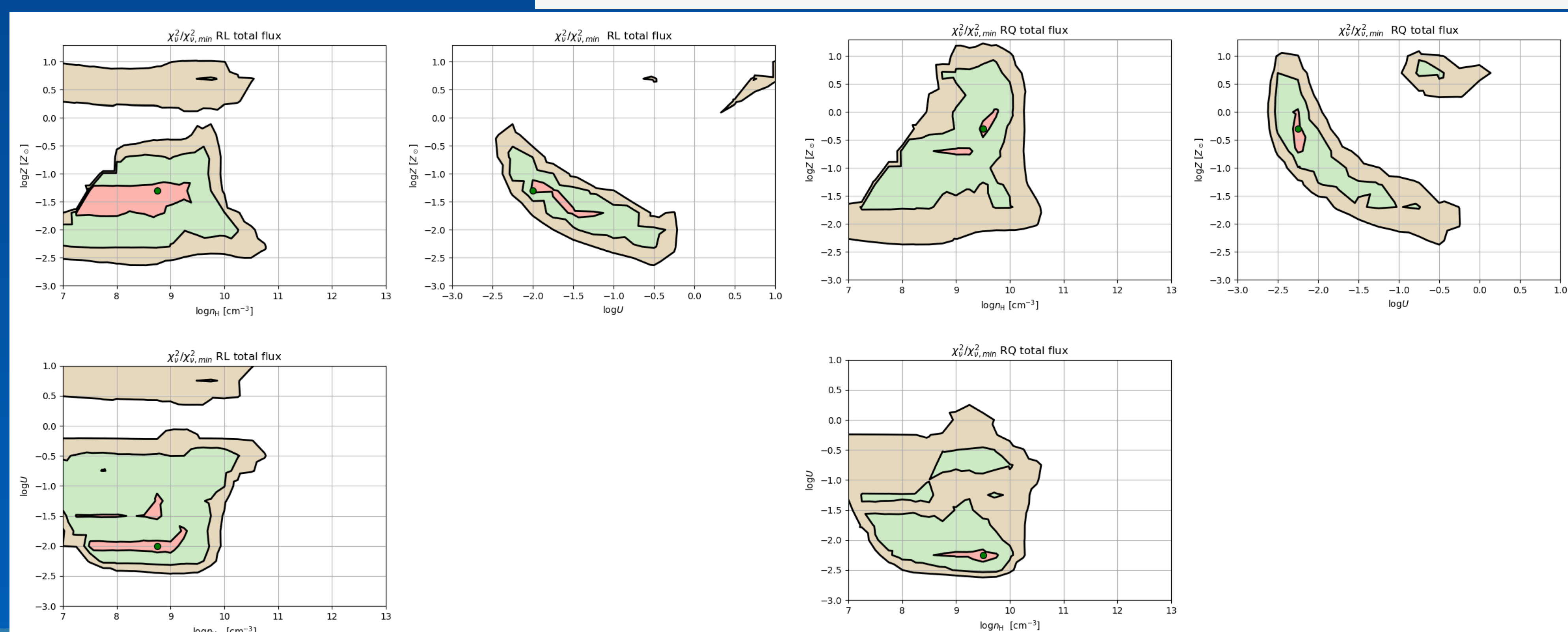

Z estimates well constrained

Population A: from modest to extreme R_{FeII}

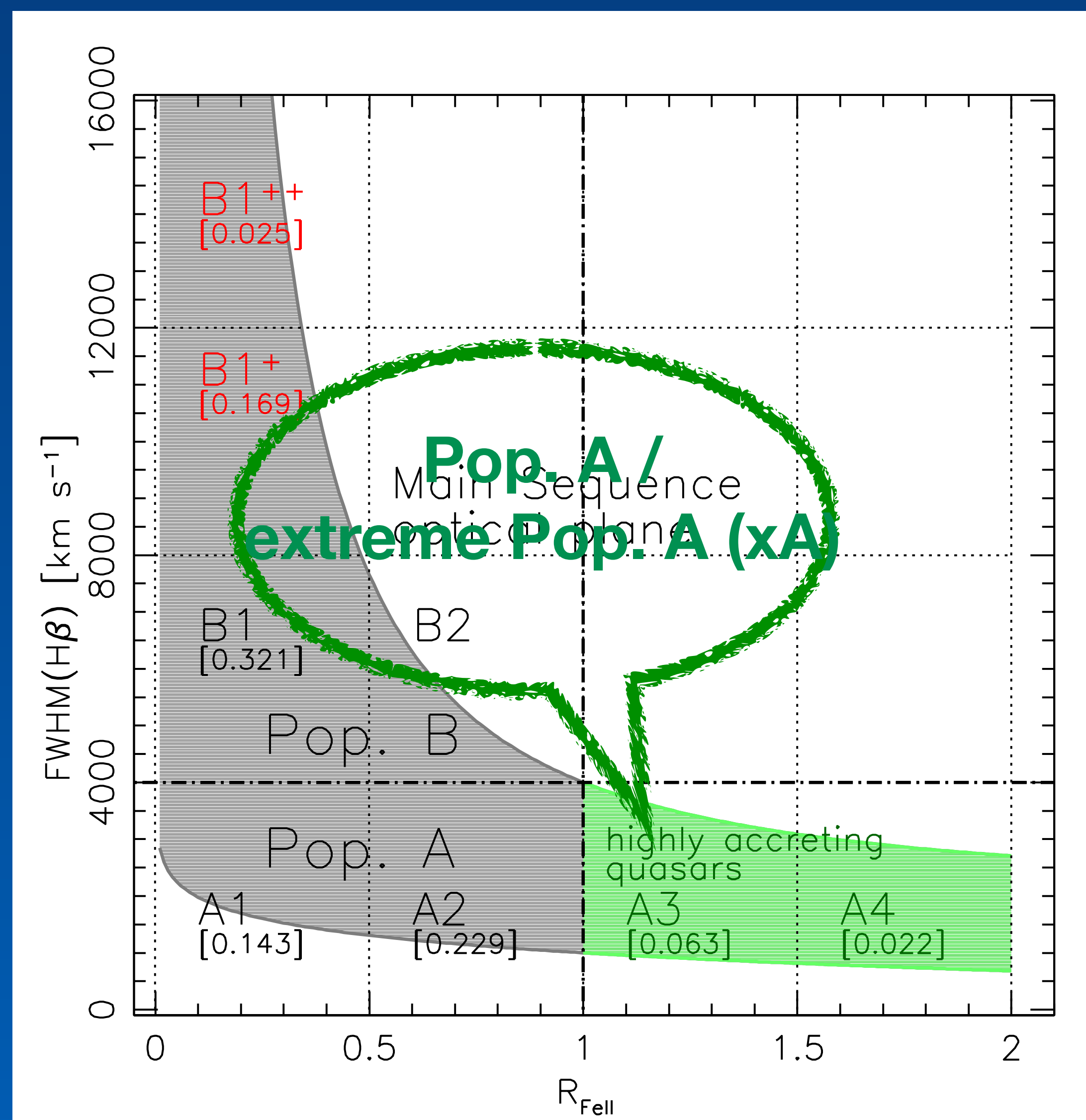

Moderate to extreme (~1) Eddington ratio

Extreme Population A sources

- Highest radiative output per unit black hole mass; most prominent wind components
- Sample of 38 SDSS quasars at redshift z~2 suitable for eventual Hβ observations in the IR
- Diagnostic line ratios
  CIVλ1549/HeIIλ1640
  AlIII λ1860/HeIIλ1640
  (SiIV+OIV])λ1400/HeIIλ1640

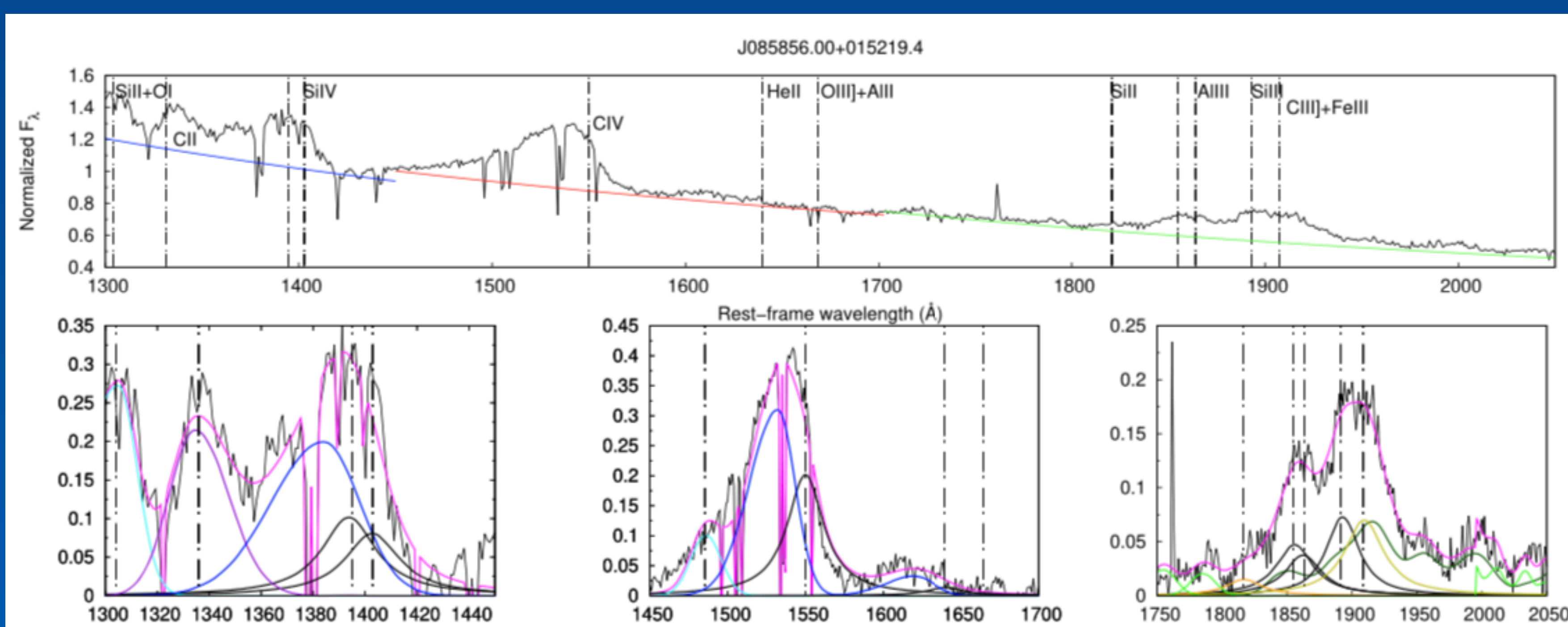

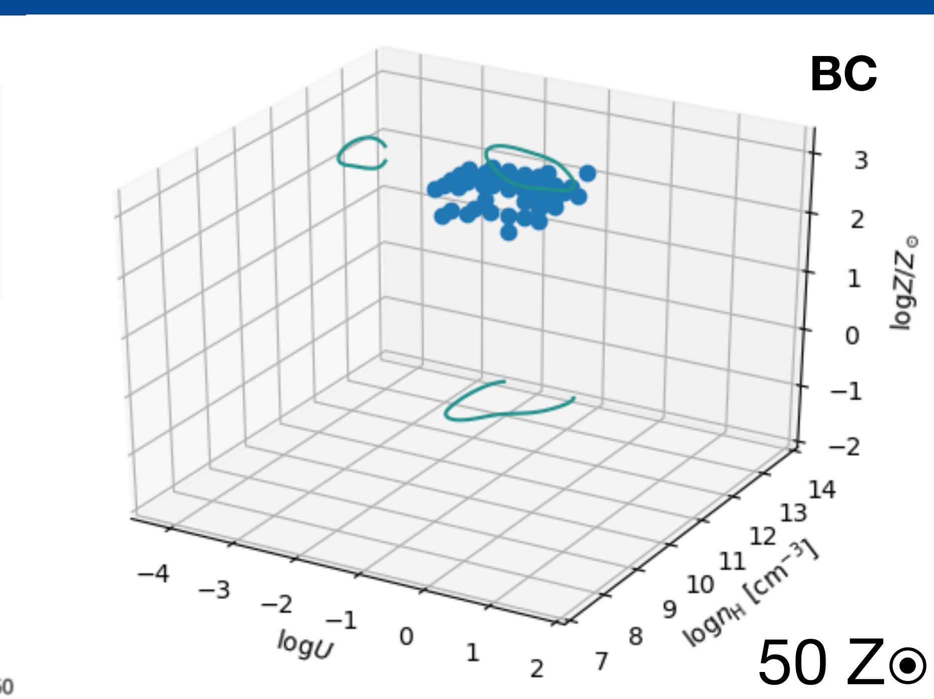

Virialized component with high Z; extreme *U* and n_H

(Negrete et al. 2012; Martínez-Aldama et al. 2018; Sniegowska et al. 2021; Garnica et al.2022

Chemical feedback from luminous AGN

- Important for galaxy evolution studies   Choi et al. 2020; Nandi et al. 2023; Molero et al. 2023

- Past and recent studies suggest high *Z* values ($\gtrsim 10\ Z_\odot$) in the BLR
  Hamann & Ferland 1992; Nagao et al. 2006; Sulentic et al. 2014; Lai et al. 2022; Xu et al. 2018; for the virialized component: Sniegowska et al. 2021; Garnica et al 2022

- Chemical abundance of the outflow component, from all measurable ratios:
  J09466-0124: X-SHOOTER VLT data; z ~ 2.2125 log*L* ~ 46; $R_{\rm FeII}$ ~0.2, Pop. A1, $Z \sim 2\text{-}5 Z_\odot$
  HE1347-2457, *z* ~ 2.534, log*L* ~ 47, $R_{\rm FeII}$ ~1.3, extreme Pop. A: $Z \sim 50\text{-}100 Z_\odot$
  Constraints on Z are especially stable; less so on U and n_H

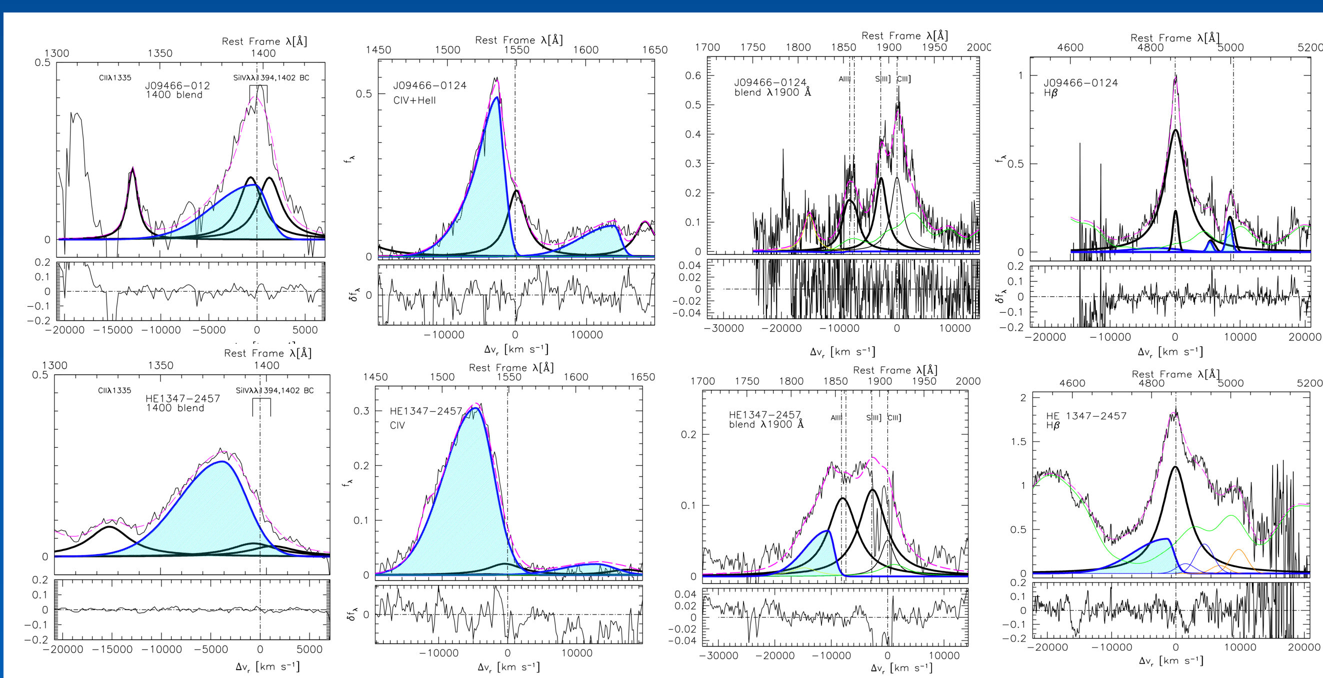

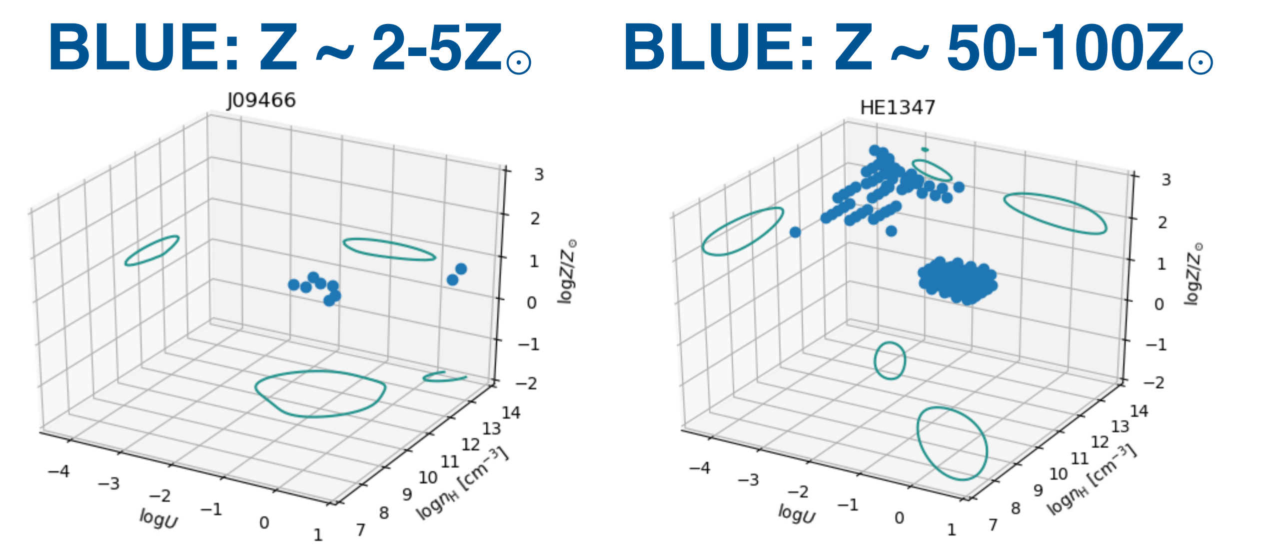

$$\chi^2_{\rm kc}(n_{\rm H}, U, Z) = \sum_{\rm i} w_{\rm ci} \left(\frac{R_{\rm kci} - R_{\rm kci,mod}(n_{\rm H}, U, Z)}{\delta R_{\rm kci}} \right)^2$$

Extreme chemical feedback from high accretors

Or Supernova pollution? Sniegowska, Garnica et al. in preparation

Differences imply over-abundances of Al and Si over C

- Z(CIV/HeII) ~ 20 $Z_{\odot}$; Z(AlIII/HeII) ~ 50-100 $Z_{\odot}$
- Systematic Z differences from different diagnostics?
- [Al/C] from Supernovæ: ~ 6 [Al/C]$_{\odot}$:

Free n_{H}, U

Fixed n_{H}, U BC

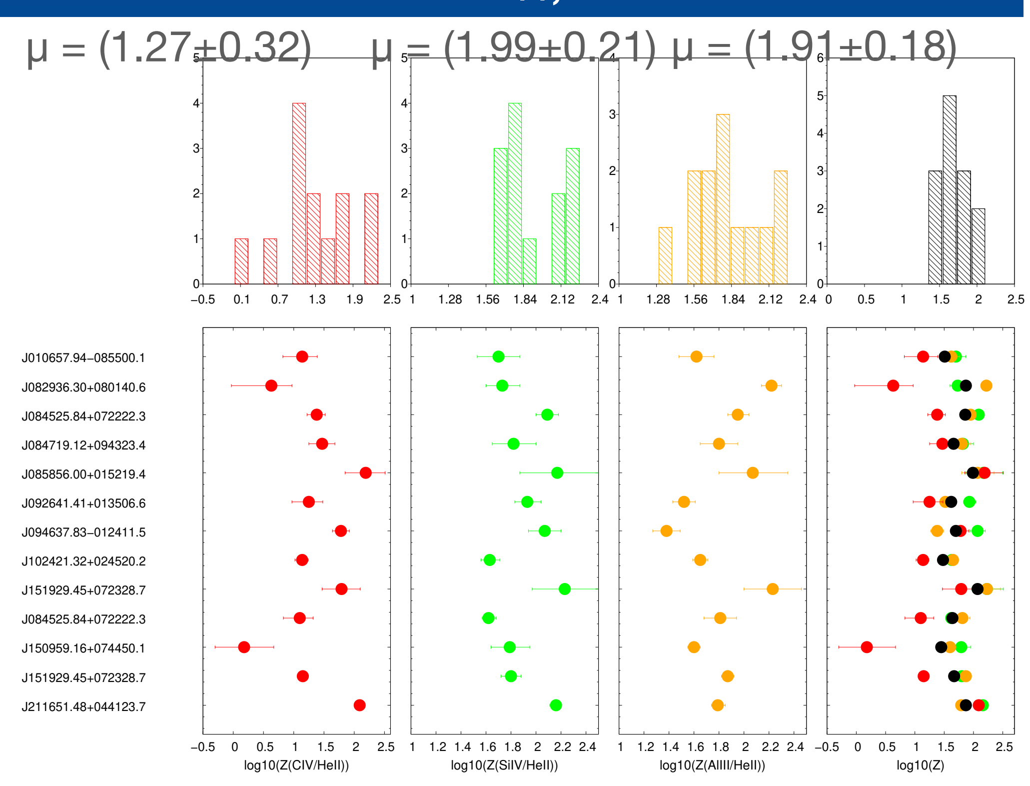

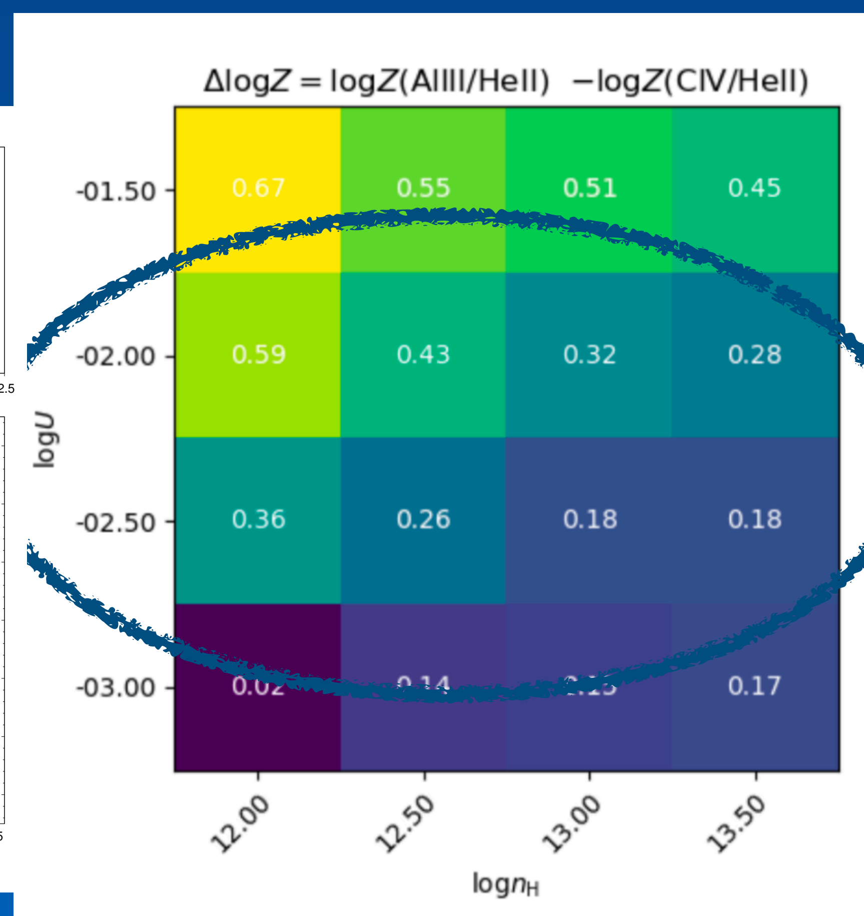

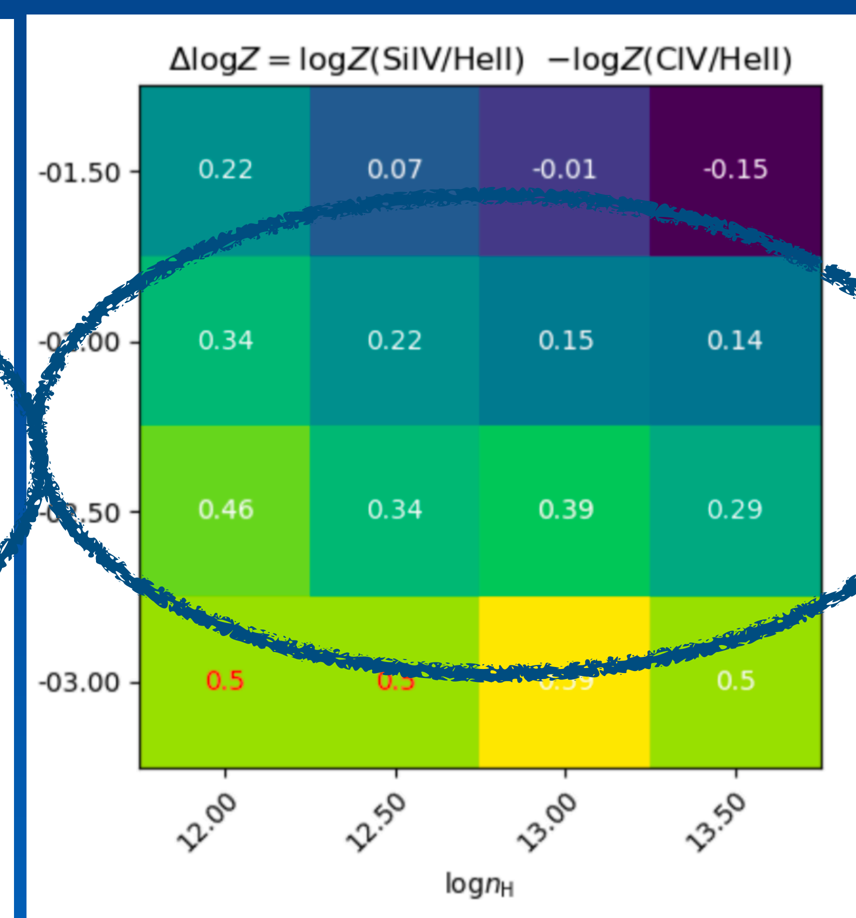

Likely pollution

(Negrete et al. 2012; Martínez-Aldama et al. 2018; Sniegowska et al. 2021; Chieffi & Limongi 2004 for SN yields

Massive, mildly ionized outflows traced by CIV and [OIII]

- Outflow dynamical parameters from CIVλ1549 can be computed knowing that the line is collisional excited like [OIII]λ5007

- HEMS: ionized gas mass flow, kinetic power and thrust are extreme for extreme Population A, as ($\propto L_{\rm line}\, v^n$)

- Kinetic power is still slightly below the values needed for host-spheroid co-evolution

  King 2003, Di Matteo et al, 2005, Hopkins et al. 2006,Hopkins & Elvis2010, Faucher-Giguère & Quataert 2012, Lapi et al. 2014, Costa et al. 2018,2020

- However, mildly ionized gas may contribute a substantial enrichment of the host: for HEMS, 100 Z⊙ ⇛ ½ gas mass due to metals. $dM/dt \sim 10\ M_\odot\ yr^{-1}$ ⇛ $M_Z \sim 5\ 10^7\ t_{7yr}\ M_\odot$

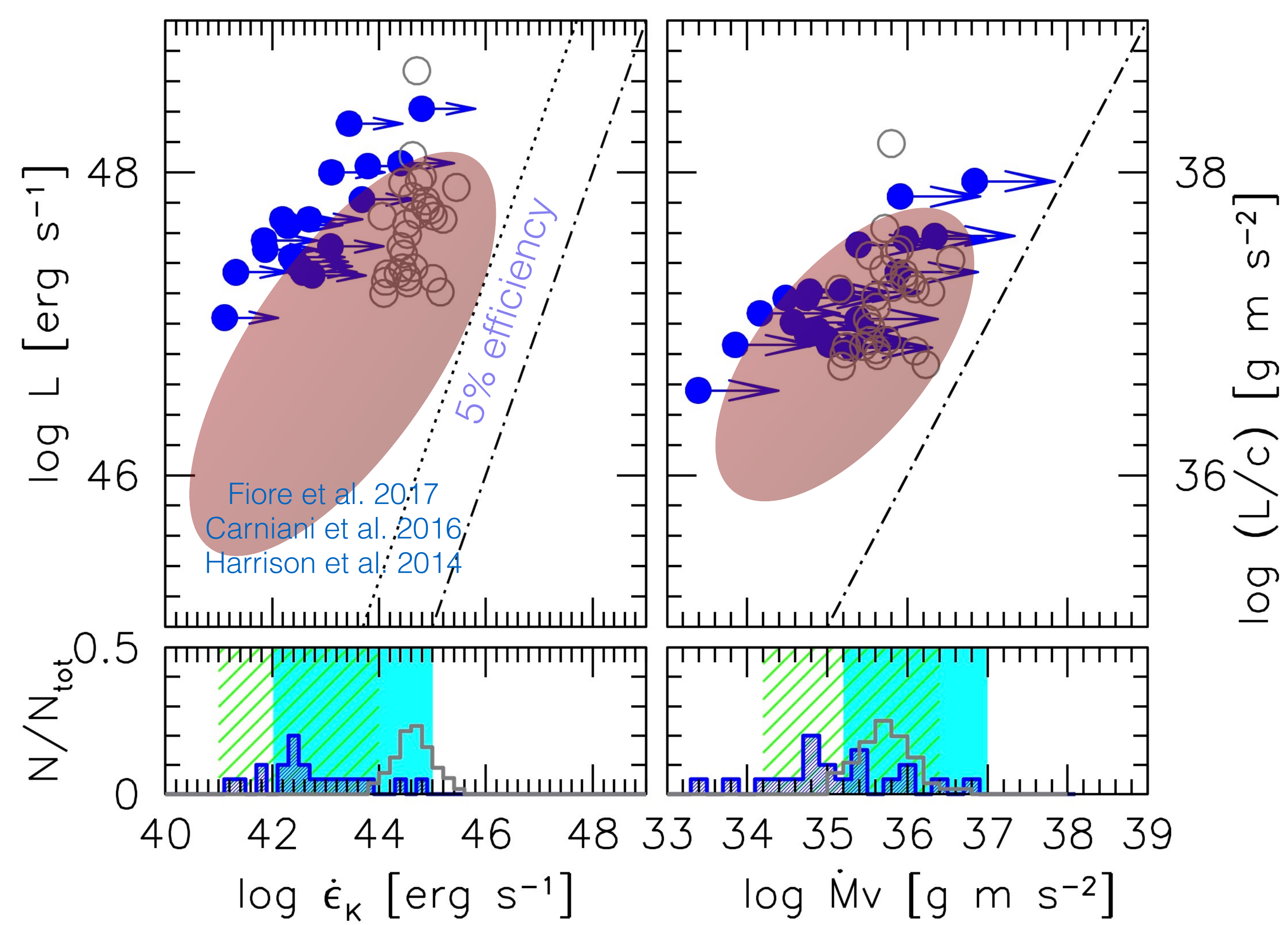

TABLE 1 | Outflow physical parameters derived for CIV and [OIII]: mass of ionized gas, mass outflow rate, thrust and kinetic power.

Parameter	Units	CIV	[OIII]
$M^{\rm ion}$	$M_\odot$	$1.9\cdot10^3\,L_{45}\left(\frac{Z}{5Z_\odot}\right)^{-1} n_9^{-1}$	$1\cdot10^7\,L_{44}\left(\frac{Z}{5Z_\odot}\right)^{-1} n_3^{-1}$
$\dot M^{\rm ion}$	$M_\odot$ yr^{-1}	$30 L_{45} v_{o,5000} r_{\rm 1pc}^{-1}\left(\frac{Z}{5Z_\odot}\right)^{-1} n_9^{-1}$	$30 L_{44} v_{o,1000} r_{\rm 1kpc}^{-1}\left(\frac{Z}{5Z_\odot}\right)^{-1} n_3^{-1}$
$\dot M^{\rm ion} k v_o$	g cm s^{-2}	$1\cdot10^{36} L_{45} k v_{o,5000}^2 r_{\rm 1pc}^{-1}\left(\frac{Z}{5Z_\odot}\right)^{-1} n_9^{-1}$	$1.9\cdot10^{35} L_{44} k v_{o,1000}^2 r_{\rm 1kpc}^{-1}\left(\frac{Z}{5Z_\odot}\right)^{-1} n_3^{-1}$
$\dot\epsilon$	erg s^{-1}	$2.4\cdot10^{44} L_{45} k^2 v_{o,5000}^3 r_{\rm 1pc}^{-1}\left(\frac{Z}{5Z_\odot}\right)^{-1} n_9^{-1}$	$9.6\cdot10^{42} L_{44} k^2 v_{o,1000}^3 r_{\rm 1kpc}^{-1}\left(\frac{Z}{5Z_\odot}\right)^{-1} n_3^{-1}$

Significant (chemical) feedback effect

* Marziani et al. 2016a; 2017 cf. Cano-Díaz et al. 2012; Carniani et al. 2015; Zakamska et al. 2016; Bischetti et al. 2017; c.f. Vietri et al. 2020

Conclusion

- There is definitely a gradient of metallicity along the quasar main sequence, from 0.1 $Z_\odot$ to several tens $Z_\odot$ from Population B to extreme Population A

- Caveats: approach dependent on spectral types, dishomogeneities in the outflow components (Pop. A) stratification in the virialized component (Pop. B), role of turbulence (minor for UV, but relevant for FeII)

- High metal content of BLR outflowing gas (from a few times $Z_\odot$ to $\lesssim 100\ Z_\odot$) suggests a chemical feedback on the host galaxy, especially from extreme Population A (candidate super-Eddington) quasars at high L

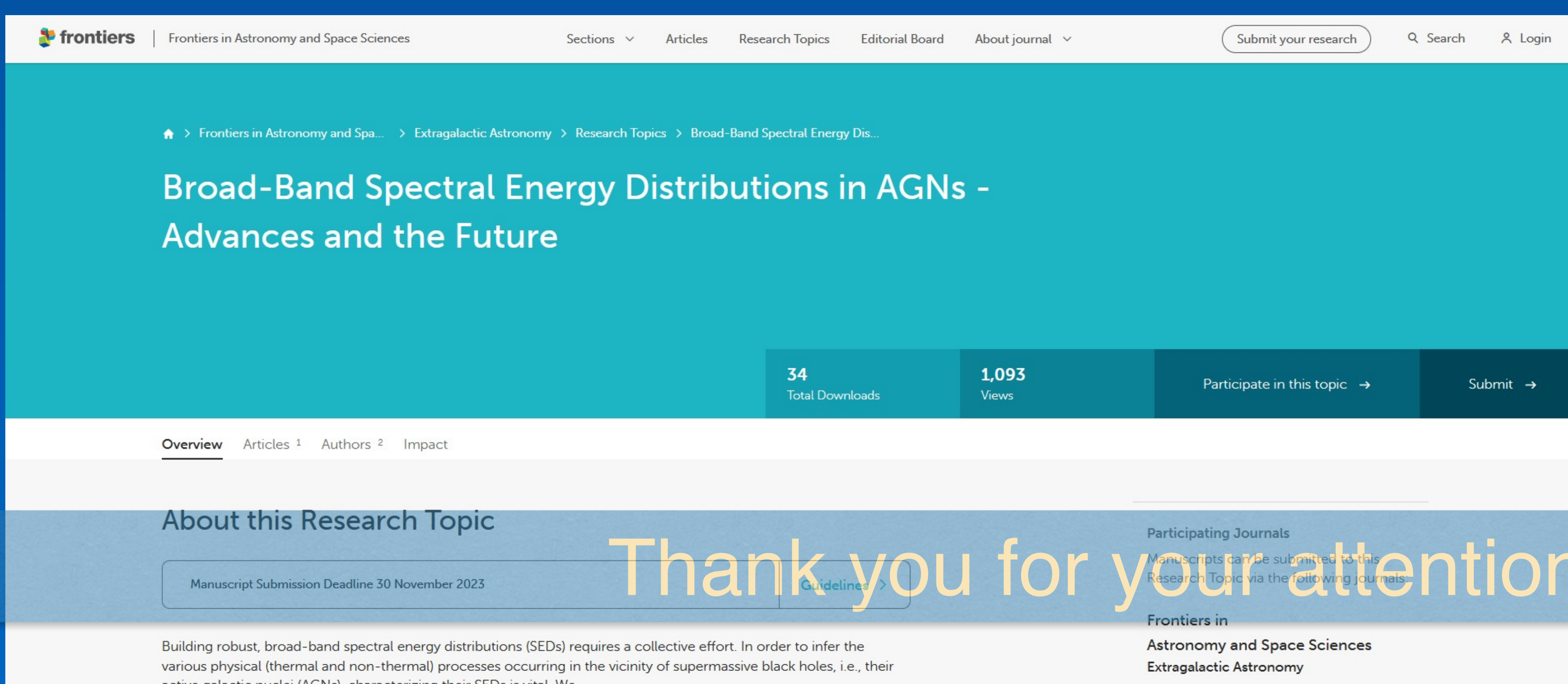

Thank you for your attention!